International Journal of Heat and Mass Transfer 202 (2023) 123721

Contents lists available at ScienceDirect

International Journal of Heat and Mass Transfer

journal homepage: www.elsevier.com/locate/hmt

The role of thermal effusivity in heat exchange between finite-sized bodies

Ankur Jain

Mechanical and Aerospace Engineering Department, University of Texas at Arlington, 500 W First St, Rm 211, Arlington, TX 76019, United States

ARTICLE INFO

Article history:
Received 22 October 2022
Revised 14 November 2022
Accepted 26 November 2022

Keywords:
Thermal effusivity
Thermal diffusivity
Interfacial heat flux
Multilayer thermal conduction
Analytical modeling

ABSTRACT

Thermal effusivity is a thermophysical property of materials that combines thermal conductivity and volumetric heat capacity. Thermal effusivity is often interpreted in terms of a body's ability to exchange heat when brought in contact with another body at a different temperature, and is relevant in thermal property measurements, such as the transient plane source method as well as in energy harvesting and thermal management. Well-known theoretical models show that thermal effusivity is the only thermophysical property that governs heat exchange between two semi-infinite bodies. In contrast, there is a lack of work on heat exchange between bodies of finite thickness, which may be a relevant consideration in several practical scenarios. This work presents an analytical solution for heat exchange between two finite bodies initially at different temperatures. The effect of thermal contact resistance is accounted for. Results from this work are shown to approach semi-infinite results when the layer thickness becomes large. It is shown that while the heat flux for finite thickness in general depends on both thermal effusivity and thermal diffusivity, exclusive dependence on effusivity may occur under certain conditions, particularly for poorly conducting materials. The sensitivity of interfacial heat flux on these thermal properties is examined in the regimes in which most materials of interest lie. The limits in which the semi-infinite approximation is reasonable are determined. A practical problem is solved as an illustration. This work improves the fundamental understanding of thermal effusivity and thermal interaction between finite-sized bodies, and may find applications in a variety of engineering problems such as thermal property measurement, energy harvesting and thermal management.

1. Introduction

Thermal conductivity k and volumetric heat capacity ρC_p are the most commonly encountered thermophysical properties of materials [1–3]. In addition, the thermal diffusivity, $\alpha = k/(\rho C_p)$ that appears in the transient energy conservation energy equation is also commonly used. In contrast, the thermal effusivity, $e = \sqrt{k\rho C_p}$ is found in the literature to a much lesser extent. Unlike other properties, effusivity does not appear explicitly in governing equations, and, therefore, its role as a fundamental thermophysical property has been open to debate.

The role of thermal effusivity is most commonly understood on the basis of perceived warmth or coldness of a body upon touch [4,5]. Using Laplace transforms technique, it can be shown that when two semi-infinite bodies initially at different temperatures (such as a human hand and a doorknob) are brought in contact with each other, the resulting temperature distribution in both layers is based on error functions [2]. Subsequently, the temperature at the interface can be shown to attain a constant value whereas the heat flux can be shown to decay as $1/\sqrt{t}$ as follows [2]:

$$T_{12,inf} = T_{2,in} + \frac{e_1}{e_1 + e_2}\left(T_{1,in} - T_{2,in}\right) \tag{1}$$

$$q_{12,inf}(\tau) = \frac{e_1 e_2}{e_1 + e_2}\frac{(T_{1,in} - T_{2,in})}{\sqrt{\pi t}} \tag{2}$$

where e_1 and e_2 are the thermal effusivities of the two bodies, while $T_{1,in}$ and $T_{2,in}$ are the initial temperatures. Eq. (2) can also be derived by starting with an error function temperature distribution in the semi-infinite bodies and applying an energy balance at the interface.

Eqs. (1) and (2) show that thermal effusivity is the only thermophysical property that governs the interfacial temperature and heat flux in this problem. The perception of coldness or warmth of an object upon touch, referred to as thermoreception [6], is based on how much heat is drawn from or supplied to the skin upon touch [7]. Therefore, Eq. (2) explains why certain materials such as metals or plastics feel relatively cold or warm, respectively, to the touch. For this reason, thermal effusivity has also been re-

E-mail address: jaina@uta.edu

https://doi.org/10.1016/j.ijheatmasstransfer.2022.123721
0017-9310/

Nomenclature

C_p	heat capacity ($Jkg^{-1}K^{-1}$)
k	thermal conductivity ($Wm^{-1}K^{-1}$)
L	layer thickness (m)
L_{ref}	reference length scale (m)
q	heat flux (Wm^{-2})
T	temperature (K)
t	time (s)
x	spatial coordinate (m)
α	diffusivity (m^2s^{-1})
e	effusivity ($Js^{-0.5}m^{-2}K^{-1}$)
ξ	non-dimensional spatial coordinate
ρ	density (kgm^{-3})
τ	non-dimensional time
θ	non-dimensional temperature
λ	eigenvalue

Subscripts

12	interface
1,2	layer number
in	initial values
ref	reference

ferred to by other names such as thermal responsivity and thermal absorptivity. Material recognition based on tactile heat transfer is an interesting application of this theory [5]. Other engineering applications where thermal effusivity has been shown to play an important role include thermal management of buildings [8], thermal performance of textiles [9], geothermal heat transfer [10], energy harvesting [11], phase change based thermal management [12], heat transfer in semiconductors [13] and periodic heat transfer processes [14].

In addition to engineering problems referenced above, thermal effusivity also often appears in thermal property measurement techniques. For example, the transient plane source method [15,16] measures thermal effusivity by measuring the interfacial temperature as a function of time when two semi-infinite samples are heated by a thin heater placed in between [17]. Thermal contact resistance at the interface can be accounted for in such measurements [18]. This technique has also been extended to account for finite thickness of the sample by dividing the time period of interest into two domains, which separately provide information about the thermal conductivity and heat capacity of the sample [19]. Other measurement techniques for thermal effusivity include hot strip [20], thermoreflectance [21], dual lock-in method [22] and photopyroelectric calorimetry [23].

The common interpretation of thermal effusivity as the property that governs heat exchange between two bodies upon touch [4] is based on the assumption that the two bodies are thermally semi-infinite, i.e., the boundaries are far enough to not influence heat transfer in the time period of interest. While this may be a reasonable assumption in several engineering problems, it is clearly not universally true. Specifically, the finite nature of the body must be accounted for when the physical size of the body is relatively small, such as in semiconductor devices [13], and/or when the time period of interest is very large, such as in geothermal problems [10]. In such cases, the interfacial temperature and heat flux given by Eqs. (1) and (2) are no longer valid, and it is unclear whether thermal effusivity continues to be the only thermophysical property governing the interfacial temperature and heat flux, or whether other properties also become relevant. As an engineering approximation, the calculation of thermal penetration depth may be used to estimate whether the semi-infinite assumption is within acceptable tolerance. However, this calculation ignores the interaction between the two bodies. A more accurate approach would be to solve the governing equations in the finite domain and determine how much the predicted interfacial heat transfer and temperature deviate from the standard values for the semi-infinite problem given by Eqs. (1) and (2). This finite thickness problem has not been sufficiently addressed in the literature. Recently, the problem of heat exchange between a finite body, such as a human hand and a semi-infinite body has been solved using the technique of Laplace transforms [24]. While this helps better understand tactile perception of large objects, it may still not be applicable in cases where both bodies are finite in size.

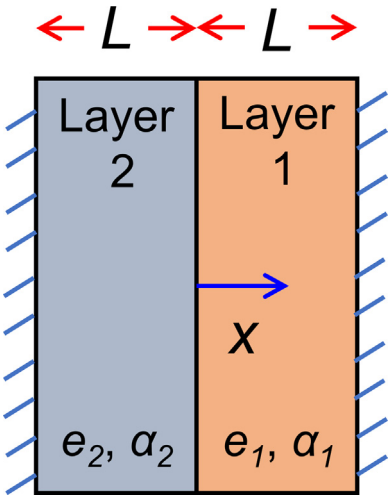

Fig. 1. Schematic of the finite-body heat exchange problem showing the geometry and coordinate system used in this work.

The present work considers and solves the problem of heat exchange between two bodies of finite size. Using multilayer diffusion analysis, expressions for transient temperature distributions in both bodies are derived in the form of infinite series. Expressions for interfacial heat flux and temperature are derived and shown to reduce to well-known results from semi-infinite analysis when the size of the bodies becomes very large. The sensitivity of interfacial heat flux on thermophysical properties in regimes representative of most materials is discussed. It is shown that while the interfacial temperature and heat flux, in general, depend both on thermal effusivity as well as another thermophysical property, such as thermal diffusivity, under certain regimes, exclusive dependence on effusivity may be possible. This work extends the heat transfer theory related to thermal effusivity by accounting for the practical but previously overlooked consideration of finite thickness. Results may help improve the design of materials and devices in a variety of engineering problems where thermal effusivity plays an important role.

2. Mathematical modeling

As shown in Fig. 1, consider the problem of one-dimensional thermal conduction in a stack of two layers of dis-similar materials and of thickness L each. The two layers are initially at distinct temperatures, $T_{1,in}$ and $T_{2,in}$, respectively. At t=0, the two layers are brought in contact with each other at $x = 0$. The other ends of both layers are assumed to be sufficiently insulated and the temperature rise low enough for heat loss to the external ambient to be negligible. A thermal contact resistance R is assumed between the layers. The layers exchange heat with each other at the interface until thermal equilibrium. The interest is in determining the temperature fields in the two bodies, $T_1(x,t)$ and $T_2(x,t)$, and thus,

the interface temperature $T_{12}(t)$ and heat flow from layer 1 to layer 2 $q_{12}(t)$ as functions of time. In particular, it is of interest to determine which thermophysical properties govern these parameters. In contrast with well-known results for semi-infinite bodies, where thermal effusivity is the only property that appears in expressions for these parameters, the interest here is to examine whether thermal effusivity remains the only thermophysical properties governing interfacial parameters in the case of finite thickness.

The two independent material thermal properties are taken to be the thermal effusivity and diffusivity, denoted by e and α, respectively. Note that other thermal properties can be written in terms of e and α. For example, the thermal conductivity may be obtained as $k = e\sqrt{\alpha}$. Subscripts 1 and 2 denote the two layers. All properties are assumed to constant, uniform and independent of temperature. Without loss of generality, it is assumed that layer 1 is hotter than layer 2 initially, i.e., $T_{1,in} > T_{2,in}$. In order to obtain a solution for this two-layer finite-body problem, it is helpful to first carry out a non-dimensionalization. Using $\theta_i = \frac{(T_i - T_{2,in})}{(T_{1,in} - T_{2,in})}$ $(i = 1,2)$, $\xi = x/L_{ref}$, $\tau = \alpha_2 t/L_{ref}^2$, $\bar{\alpha}_1 = \alpha_1/\alpha_2$, $\bar{e}_1 = e_1/e_2$, $\bar{L} = L/L_{ref}$, $\bar{R} = e_2\sqrt{\alpha_2}R/L_{ref}$, where L_{ref} is an arbitrary reference length scale, the following energy conservation equations for temperature fields in the two layers may be obtained:

$$\frac{\partial^2\theta_1}{\partial\xi^2} = \frac{1}{\bar{\alpha}_1}\frac{\partial\theta_1}{\partial\tau} \qquad \left(0 < \xi < \bar{L}\right) \tag{3}$$

$$\frac{\partial^2\theta_2}{\partial\xi^2} = \frac{\partial\theta_2}{\partial\tau} \qquad \left(-\bar{L} < \xi < 0\right) \tag{4}$$

The ends of the layers are assumed to be adiabatic, while temperature continuity and heat flux conservation is assumed at the interface. This results in the following boundary and interface conditions:

$$\frac{\partial\theta_1}{\partial\xi} = 0 \qquad \left(\xi = \bar{L}\right) \tag{5}$$

$$\frac{\partial\theta_2}{\partial\xi} = 0 \qquad \left(\xi = -\bar{L}\right) \tag{6}$$

$$\theta_1 = \theta_2 + \bar{e}_1\sqrt{\bar{\alpha}_1}\bar{R}\frac{\partial\theta_1}{\partial\xi} \qquad (\xi = 0) \tag{7}$$

$$\bar{e}_1\sqrt{\bar{\alpha}_1}\frac{\partial\theta_1}{\partial\xi} = \frac{\partial\theta_2}{\partial\xi} \qquad (\xi = 0) \tag{8}$$

Note that in Eq. (8) above, thermal conductivity is expressed as $\bar{k}_1 = \bar{e}_1\sqrt{\bar{\alpha}_1}$ in order to write the equations only in terms of two properties – effusivity and diffusivity.

Finally, the initial condition is given by

$$\theta_1 = 1;\ \theta_1 = 0 \qquad (\tau = 0) \tag{9}$$

Therefore, the non-dimensional problem comprises layers 1 and 2 at a unit and zero temperature, respectively at the initial time. Note that an arbitrary reference length scale L_{ref} is used for non-dimensionalization instead of the layer thickness L in order to explicitly preserve the layer thickness in the form of $\bar{L}$. This makes it easier to examine the impact of finite layer thickness on interfacial temperature and heat flux, and to compare with the semi-infinite problem.

The problem described by Eqs. (3)–(9) is a multilayer diffusion problem [1]. The solution may be written in the form of an infinite series, the eigenvalues and various coefficients of which may be obtained using the boundary and interface conditions, as well as the principle of quasi-orthogonality [25] in conjunction with the initial condition. The following general form for the temperature distributions may be written

$$\theta_1(\xi,\tau) = c_0 + \sum_{n=1}^{\infty} c_n\left[A_{1,n}\cos\left(\frac{\lambda_n\left(\bar{L}-\xi\right)}{\sqrt{\bar{\alpha}_1}}\right) + B_{1,n}\sin\left(\frac{\lambda_n\left(\bar{L}-\xi\right)}{\sqrt{\bar{\alpha}_1}}\right)\right]\exp\left(-\lambda_n^2\tau\right) \tag{10}$$

$$\theta_2(\xi,\tau) = c_0 + \sum_{n=1}^{\infty} c_n\left[A_{2,n}\cos\left(\lambda_n\left(\bar{L}+\xi\right)\right) + B_{2,n}\sin\left(\lambda_n\left(\bar{L}+\xi\right)\right)\right]\exp\left(-\lambda_n^2\tau\right) \tag{11}$$

Note the Eqs. (10) and (11) satisfy the respective governing energy equations. The c_0 term appearing in both equations corresponds to the zero eigenvalue, which must be explicitly included in this problem because both external boundary conditions are adiabatic [1]. c_0 may be interpreted as the steady state temperature that both layers equilibrate to at large time, and may be determined by noting that the total energy at large time must equal the total initial energy in this perfectly insulated two-layer geometry. This can be shown to result in

$$c_0 = \frac{\bar{e}_1}{\bar{e}_1 + \sqrt{\bar{\alpha}_1}} \tag{12}$$

In order to satisfy the boundary conditions given by Eqs. (5) and (6), it can be seen that $B_{1,n} = B_{2,n} = 0$. Further, the use of the interface conditions shows that

$$A_{2,n}\cos\left(\lambda_n\bar{L}\right) = A_{1,n}\left[\cos\left(\lambda_n\bar{L}/\sqrt{\bar{\alpha}_1}\right) - \bar{e}_1\bar{R}\lambda_n\sin\left(\lambda_n\bar{L}/\sqrt{\bar{\alpha}_1}\right)\right] \tag{13}$$

$$\bar{e}_1 A_{1,n}\sin\left(\lambda_n\bar{L}/\sqrt{\bar{\alpha}_1}\right) = -A_{2,n}\sin\left(\lambda_n\bar{L}\right) \tag{14}$$

Dividing Eq. (13) by Eq. (14) results in the following eigenequation, the positive roots of which determine the eigenvalues λ_n:

$$\cot\left(\frac{\lambda_n\bar{L}}{\sqrt{\bar{\alpha}_1}}\right) + \bar{e}_1\cot\left(\lambda_n\bar{L}\right) - \bar{e}_1\bar{R}\lambda_n = 0 \tag{15}$$

Therefore, the temperature distributions may be written in simpler form as

$$\theta_1(\xi,\tau) = c_0 + \sum_{n=1}^{\infty} c_n\cos\left(\frac{\lambda_n\left(\bar{L}-\xi\right)}{\sqrt{\bar{\alpha}_1}}\right)\exp\left(-\lambda_n^2\tau\right) \tag{16}$$

$$\theta_2(\xi,\tau) = c_0 + \sum_{n=1}^{\infty} c_n\frac{\cos\left(\lambda_n\bar{L}/\sqrt{\bar{\alpha}_1}\right) - \bar{e}_1\bar{R}\lambda_n\sin\left(\lambda_n\bar{L}/\sqrt{\bar{\alpha}_1}\right)}{\cos\left(\lambda_n\bar{L}\right)}\cos\left(\lambda_n\left(\bar{L}+\xi\right)\right)\exp\left(-\lambda_n^2\tau\right) \tag{17}$$

Finally, the use of the initial condition along with the principle of orthogonality results in the following expression, which has been simplified using the eigenequation

$$c_n = \frac{\bar{e}_1\sqrt{\bar{\alpha}_1}\int_0^{\bar{L}}\cos\left(\frac{\lambda_n\left(\bar{L}-\xi\right)}{\sqrt{\bar{\alpha}_1}}\right)d\xi}{\bar{e}_1\sqrt{\bar{\alpha}_1}\int_0^{\bar{L}}\cos^2\left(\frac{\lambda_n\left(\bar{L}-\xi\right)}{\sqrt{\bar{\alpha}_1}}\right)d\xi + \int_{-\bar{L}}^{0}\left[\frac{\cos\left(\lambda_n\bar{L}/\sqrt{\bar{\alpha}_1}\right) - \bar{e}_1\bar{R}\lambda_n\sin\left(\lambda_n\bar{L}/\sqrt{\bar{\alpha}_1}\right)}{\cos\left(\lambda_n\bar{L}\right)}\right]^2\cos^2\left(\lambda_n\left(\bar{L}+\xi\right)\right)d\xi} \tag{18}$$

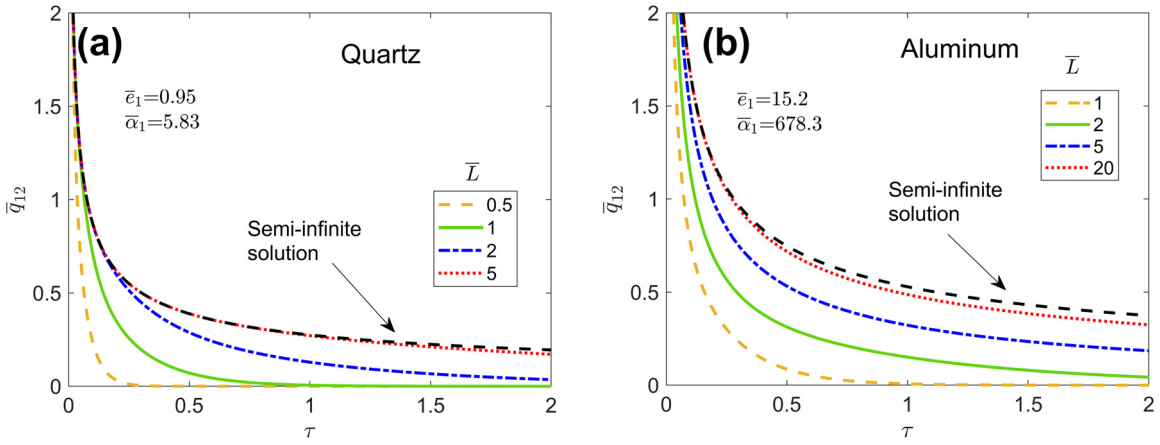

Fig. 2. Non-dimensional interfacial heat flux $\bar{q}_{12}$ as a function of time for different values of layer thickness $\bar{L}$. Two material pairs are considered: (a) $\bar{e}_1 = 0.95$, $\bar{\alpha}_1 = 5.83$ (quartz and human hand) and (b) $\bar{e}_1 = 15.2$, $\bar{\alpha}_1 = 678.3$ (aluminum and human hand). For comparison, the interfacial heat flux curves for the respective semi-infinite problems are also shown.

This results in the following expressions for the two quantities of specific interest – the interface temperature and interface heat flux (from layer 1 to layer 2) – as functions of time

$$\theta_{12}(\tau) = \theta_1(0,\tau) = c_0 + \sum_{n=1}^{\infty} c_n \cos\left(\frac{\lambda_n \bar{L}}{\sqrt{\bar{\alpha}_1}}\right) \exp\left(-\lambda_n^2 \tau\right) \tag{19}$$

$$\bar{q}_{12}(\tau) = \bar{e}_1 \sqrt{\bar{\alpha}_1} \left(\frac{\partial \theta_1}{\partial \xi}\right)_{\xi=0} = \bar{e}_1 \sum_{n=1}^{\infty} c_n \lambda_n \sin\left(\frac{\lambda_n \bar{L}}{\sqrt{\bar{\alpha}_1}}\right) \exp\left(-\lambda_n^2 \tau\right) \tag{20}$$

It is of interest to compare these characteristics of heat exchange between bodies of finite thickness with the semi-infinite problem, for which, the interface temperature and heat flux are given by Eqs. (1) and (2), respectively. Note that for the semi-infinite problem, the interface temperature remains constant with time, and thermal effusivity is the only property that appears in the expressions for the interface temperature and flux. In comparison, it is of interest to determine if the same holds in the present case or not.

3. Results and discussion

3.1. Comparison with semi-infinite solution

It is of interest to compare the finite thickness solution derived in Section 2 with the well-known semi-infinite solution. Such comparison may be carried out in terms of the interfacial heat flux $\bar{q}_{12}$ or the interfacial temperature θ_{12}, both as functions of time. Fig. 2 presents this comparison for the interfacial heat flux. For two representative materials – quartz and aluminum – coming in contact with human skin (mimicking the process of touching an object made of these materials), Fig. 2(a) and 2(b) plot the respective heat flux curves as functions of time for multiple values of the layer thickness $\bar{L}$. Standard material properties are assumed [3]. For generality, the plots are presented in non-dimensional form. The semi-infinite solution given by Eq. (2) is also plotted for reference. Unless stated otherwise, perfect thermal contact is assumed between the two materials in this and subsequent Figures. As expected, the interfacial heat flux reduces as time increases, and the curves for the finite thickness cases are lower than the semi-infinite curve. This is mainly because of greater thermal energy content available in a thicker layer that can sustain greater interfacial heat flux for a longer time. As expected, the finite thickness curves shift upwards and approach the semi-infinite curve as the layer thickness increases. For example, Fig. 2(a) shows that for quartz, $\bar{L} = 5$ is practically coincident with the semi-infinite curve in the time period considered here.

It is also interesting to note that even curves for relatively small layer thickness are in excellent agreement with the semi-infinite curve at small times. For example, the $\bar{L} = 2$ curve in Fig. 2(a) is coincident with the semi-infinite curve up to around $\tau = 0.2$, beyond which, it begins to deviate. This is because for a given layer thickness, the semi-infinite assumption is still valid at small times, by when the thermal wave has not yet reached the boundaries, and, therefore, thermal conduction occurs in an apparently semi-infinite medium. As expected, as $\bar{L}$ grows, the time period of good agreement with the semi-infinite solution also goes up due to greater space available, and, therefore, greater time taken by the thermal diffusion wave to reach the boundary.

Fig. 2(a) and 2(b) may also be used to compare the performance of two distinct materials – quartz and aluminum – that are representative of poorly conductive and highly conductive materials, respectively. For the same layer thickness, these plots show greater heat flux for aluminum than quartz, similar to the semi-infinite case. Therefore, the perception of a metal being colder to the human touch than a non-metal due to greater heat flux is also valid for a finite thickness geometry. Similar to Fig. 2(a) for quartz, the curves in Fig. 2(b) for aluminum also approach the semi-infinite curve as the layer thickness increases. However, it is seen that in this case, it takes a larger thickness to approach the semi-infinite curve. For example, while the $\bar{L} = 5$ curve for quartz is practically identical to the semi-infinite curve, the two are not in similarly good agreement for aluminum, which is seen to require an even greater thickness for the finite thickness model to approach the semi-infinite model. This is primarily due to the greater diffusivity of metals compared to non-metals, which causes the external boundary condition to play a more important role, even for the same thickness.

Fig. 3 presents a similar comparison between the finite thickness model presented in Section 2 and the standard semi-infinite model in terms of the interface temperature as a function of time. While the interface temperature is invariant with time for the semi-infinite model, as given by Eq. (1), in the case of the finite thickness model, it is found that the interface temperature reaches its steady state value c_0 given by Eq. (12) quite rapidly. For this reason, comparison between finite thickness and semi-infinite models in terms of the interface temperature are plotted over a very short time period. These comparison plots are presented in Fig. 3(a) and

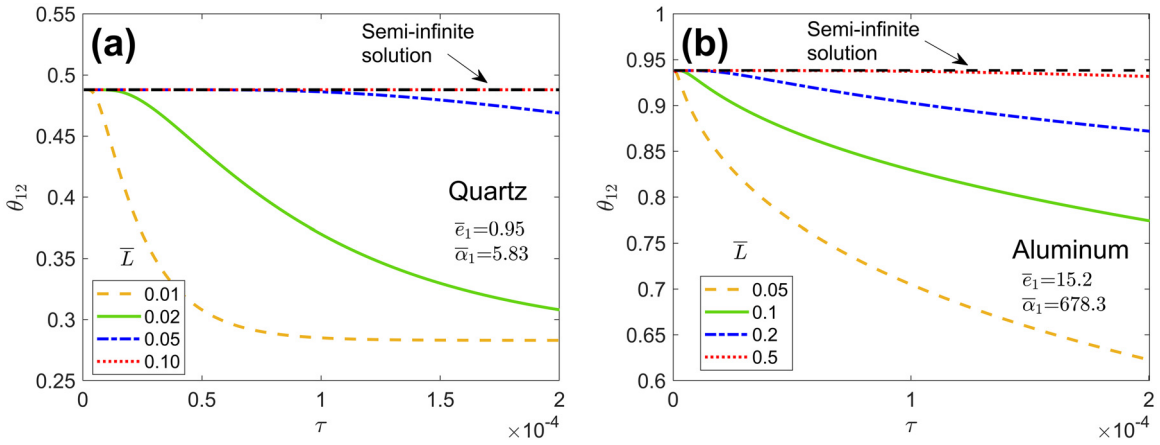

Fig. 3. Non-dimensional interfacial temperature θ_{12} as a function of time for different values of layer thickness $\bar{L}$. Two material pairs are considered: (a) $\bar{e}_1 = 0.95$, $\bar{\alpha}_1 = 5.83$ (quartz and human hand) and (b) $\bar{e}_1 = 15.2$, $\bar{\alpha}_1 = 678.3$ (aluminum and human hand). For comparison, the interfacial temperatures for the respective semi-infinite problems are also shown.

3(b) for quartz and aluminum, respectively. These plots show that in case of quartz, the interface temperature predicted by the finite thickness model is quite close to the semi-infinite model even when the layer thickness is quite small. In contrast, there is large disagreement between the two in the case of aluminum when the layer thickness is relatively small. In both cases, the interface temperature undergoes a rapid evolution at small times, and reaches a value lower than the one predicted by the semi-infinite model. When the layer thickness is larger, $\bar{L} = 0.1$ and $\bar{L} = 0.5$ for quartz and aluminum, respectively, the two models begin to agree nearly exactly with each other in the time period considered here.

3.2. Sensitivity of interfacial heat flux to thermal effusivity and thermal diffusivity

It is of interest to determine whether the interfacial heat flux in case of finite thickness layers remains sensitive only to the thermal effusivity, as is well known to be the case for semi-infinite bodies (Eq. (2)). Eq. (20) provides an analytical expression for the interfacial heat flux for finite thickness. Both $\bar{e}_1$ and $\bar{\alpha}_1$ appear in Eq. (20), and, in addition, the eigenvalues λ_n and coefficients c_n implicitly depend on both thermal effusivity and diffusivity. Yet, it is possible that in certain regimes, $\bar{q}_{12}$ may be only weakly sensitive to one of the properties.

Before investigating this in detail, it is helpful to understand the ranges of $\bar{e}_1$ and $\bar{\alpha}_1$ for common materials. Fig. 4 presents a plot of $\bar{e}_1$ and $\bar{\alpha}_1$ for common materials, ranging from poorly conducting materials such as plastics to highly conducting metals. Note that the properties of water at 300 K and 1 atm are used for non-dimensionalization. Fig. 4 shows that even though thermal diffusivity and effusivity are, in principle, independent of each other, yet, most materials tend to fall in one of two categories – low $\bar{e}_1$ and $\bar{\alpha}_1$ materials, which are mostly non-metals, or high $\bar{e}_1$ and $\bar{\alpha}_1$ materials, which are mostly metals. It is unlikely, based on the definitions of $\bar{e}_1$ and $\bar{\alpha}_1$ in terms of thermal conductivity and heat capacity that a material may have low $\bar{e}_1$ but high $\bar{\alpha}_1$, or high $\bar{e}_1$ but low $\bar{\alpha}_1$.

In order to investigate the sensitivity of interfacial heat flux on the thermophysical properties for finite thickness, $\bar{q}_{12}$ at a specific time is plotted as a function of the thermal properties. A number of layer thicknesses are considered, and the analysis is carried out for both thermal effusivity as well as thermal diffusivity. Fig. 5 presents these plots for examining the dependence on thermal diffusivity while the thermal effusivity is held constant. Plots at $\tau = 0.2$ corresponding to $\bar{e}_1 = 0.3$, representative of poorly conducting materials and $\bar{e}_1 = 12.0$, representative of highly conducting materials, both relative to human skin are presented in Fig. 5(a) and 5(b), respectively. Based on the findings in Fig. 4, the $\bar{\alpha}_1$ region in which most practical materials do not appear has been shaded out in both Fig. 5(a) and 5(b). Curves corresponding to the semi-infinite model are also presented in Fig. 5(a) and 5(b) for comparison. These curves are flat lines because of zero dependence of the interfacial heat flux on thermal diffusivity, per Eq. (1).

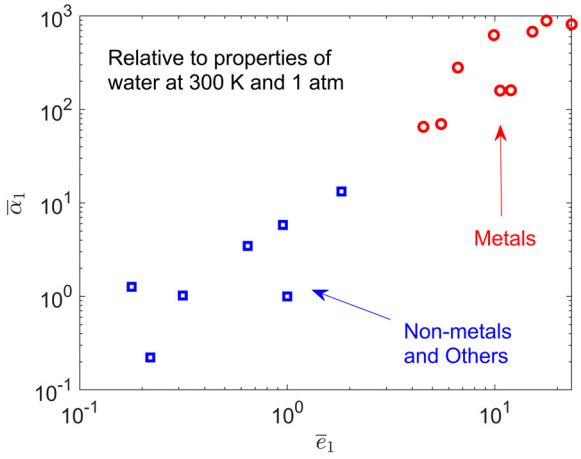

Fig. 4. Plot showing a number of common materials in the $\bar{e}_1$-$\bar{\alpha}_1$ space, relative to properties of water at 300 K and 1 atm.

For each layer thickness considered in Fig. 5, $\bar{q}_{12}$ is found to be insensitive to $\bar{\alpha}_1$ for very small and very large values of $\bar{\alpha}_1$, while exhibiting strong sensitivity at intermediate values. The reduced sensitivity at large $\bar{\alpha}_1$ is primarily because most of the thermal energy has already been conducted due to high diffusivity and the two layers are now close to thermal equilibrium, leading to $\bar{q}_{12}$ becoming nearly zero. The reduced sensitivity at small $\bar{\alpha}_1$ is because at a small enough diffusivity, the finite thickness body behaves like a semi-infinite body due to the thermal diffusive wave being limited to within the body. As the layer thickness increases, the lack of sensitivity expands to increasingly larger values of $\bar{\alpha}_1$, also due to diffusion being limited to within the body, and eventually, at a large enough value of the layer thickness, the results for the finite thickness body become completely insensitive to $\bar{\alpha}_1$ and identical to the semi-infinite model. Fig. 5(a) and 5(b) also show that the

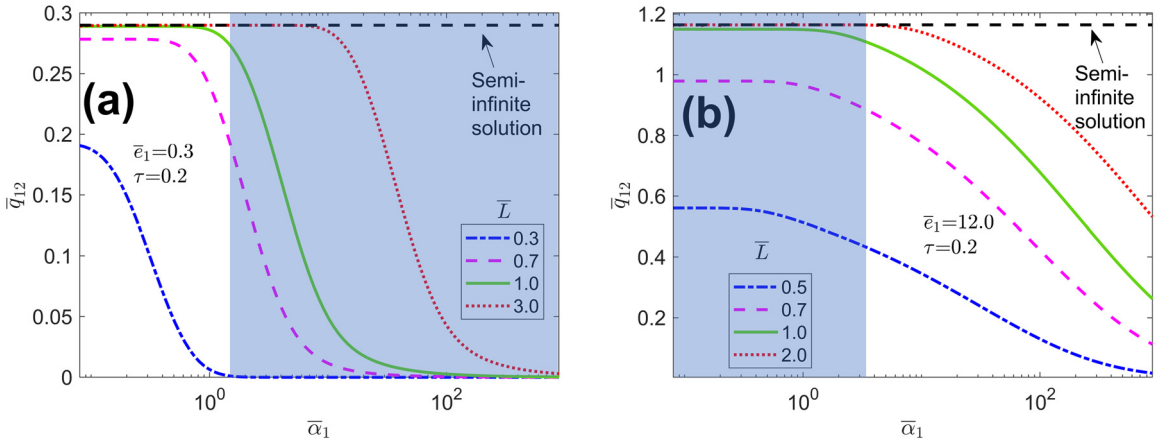

Fig. 5. Interfacial heat flux $\bar{q}_{12}$ at $\tau = 0.2$ as a function of $\bar{\alpha}_1$ for multiple layer thicknesses. Plots are shown for (a) $\bar{e}_1 = 0.3$, (b) (a) $\bar{e}_1 = 12.0$. The curves corresponding to the semi-infinite solution are also shown for reference. For the given value of $\bar{e}_1$, the $\bar{\alpha}_1$ region in which most practical materials do not appear has been shaded out.

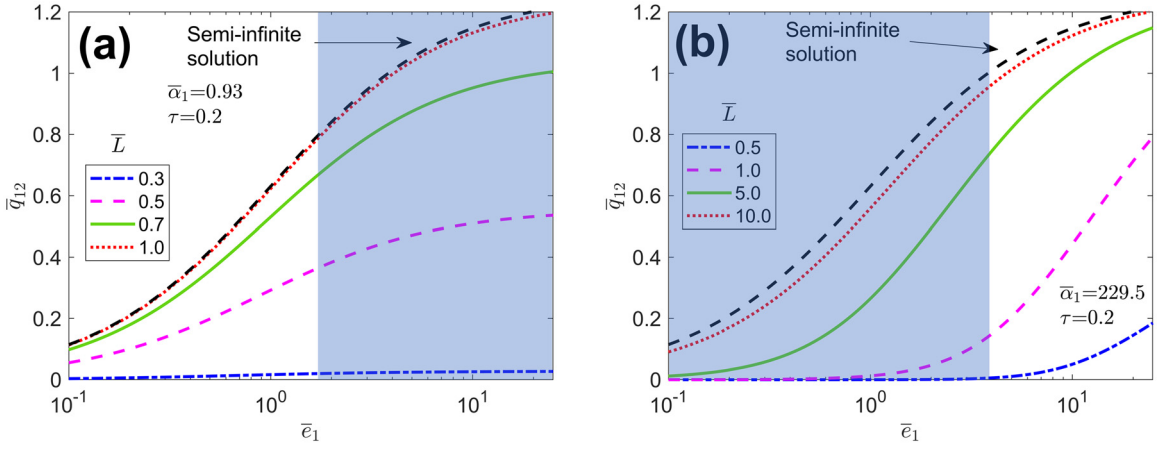

Fig. 6. Interfacial heat flux $\bar{q}_{12}$ at $\tau = 0.2$ as a function of $\bar{e}_1$ for multiple layer thicknesses. Plots are shown for (a) $\bar{\alpha}_1 = 0.93$, (b) $\bar{\alpha}_1 = 12.0$. The curves corresponding to the semi-infinite solution are also shown for reference. For the given value of $\bar{\alpha}_1$, the $\bar{e}_1$ region in which most practical materials do not appear has been shaded out.

intermediate region of high sensitivity is much broader when the effusivity is large.

A similar analysis for sensitivity of the interfacial heat flux is presented in terms of thermal effusivity in Fig. 6(a) and 6(b) for two values of the thermal diffusivity, $\bar{\alpha}_1 = 0.93$ and $\bar{\alpha}_1 = 229.5$, respectively. These plots show, similar to the semi-infinite body, very high sensitivity to $\bar{e}_1$ at small values regardless of the value of thermal diffusivity. The sensitivity reduces as $\bar{e}_1$ increases, although, unlike the case of $\bar{\alpha}_1$, it never becomes completely insensitive. With reference to the common range of $\bar{e}_1$ and $\bar{\alpha}_1$ shown in Fig. 4, the plots shown in Fig. 6(a) and 6(b) imply that measuring the interfacial heat flux to determine the thermal effusivity of the material is likely to work much better for non-metallic materials that have both low effusivity and diffusivity. Finally, note that similar to Fig. 2, the curves in Fig. 6 approach the semi-infinite curve when the layer thickness becomes sufficiently large.

In order to comprehensively understand the dependence of $\bar{q}_{12}$ on $\bar{e}_1$ and $\bar{\alpha}_1$, a colorplot of $\bar{q}_{12}$ at $\tau = 0.2$ in the $\bar{e}_1$-$\bar{\alpha}_1$ space is presented in Fig. 7. Unlike the semi-infinite body, in which the interfacial heat flux is a function of only $\bar{e}_1$, in the finite thickness case, the interfacial heat flux in general depends on both $\bar{e}_1$ and $\bar{\alpha}_1$. Note that most materials are located along the antidiagonal of this plot, with metals located in the top right quadrant (high $\bar{e}_1$ and $\bar{\alpha}_1$) and non-metals in the bottom left quadrant (low $\bar{e}_1$ and $\bar{\alpha}_1$). The bottom half of this colorplot shows that for low diffusivity materials such as plastics and other insulators, the interfacial heat flux may be reasonably considered to be independent of diffusivity since the iso-$\bar{q}_{12}$ curves are vertical in that region. This is, however, not the case for high diffusivity materials such as metals where the iso-$\bar{q}_{12}$ curves are tilted, thus indicating sensitivity to both $\bar{e}_1$ and $\bar{\alpha}_1$. The results discussed above are specific for the particular layer

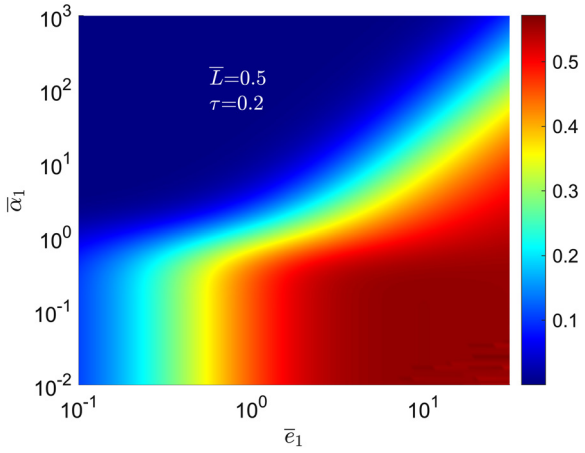

Fig. 7. Sensitivity of interfacial heat flux to thermophysical properties: $\bar{q}_{12}$ in the $\bar{e}_1$-$\bar{\alpha}_1$ space for $\bar{L} = 0.5$ and $\tau = 0.2$.

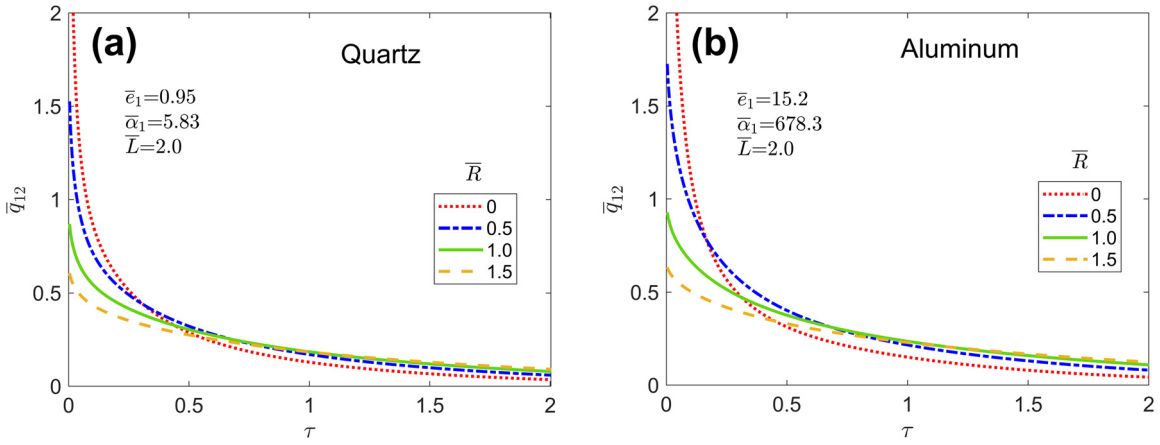

Fig. 8. Effect of thermal contact resistance: Nondimensional interfacial heat flux $\bar{q}_{12}$ as a function of time for different values of thermal contact resistance $\bar{R}$ for contact between (a) human hand and quartz, and (b) human hand and aluminum. A thickness of $\bar{L} = 2.0$ is used in both cases.

thickness and time used in this plot. At smaller thicknesses and/or at larger times, the departure from exclusive dependence on $\bar{e}_1$ is expected to become even more pronounced. On the other hand, as the layer thickness grows, the behavior of the finite-thickness body is expected to get closer and closer to that of a semi-infinite geometry. This may be the regime in which measurement of thermal effusivity of a finite-sized body may be most effective.

3.3. Effect of thermal contact resistance

While the discussion of the finite thickness problem in previous sections assumed perfect thermal contact, in some cases, thermal contact resistance at the interface between the two layers may influence heat exchange between the two. This phenomenon, represented in the mathematical model by the non-dimensional thermal contact resistance $\bar{R}$ may be important in practical scenarios, for example, when the interface between the layers is rough, or when the two materials have very different phonon transport characteristics. Fig. 8 investigates the impact of $\bar{R}$ on $\bar{q}_{12}$ as a function of time. Plots are presented for quartz and aluminum in Fig. 8(a) and 8(b), respectively. In each case, a constant thickness $\bar{L} = 2.0$ is assumed. Both plots show that increasing the thermal contact resistance reduces the heat flux at small times while increasing it at larger times. This is because of the impedance to heat flow offered by the interfacial thermal contact resistance, per Eq. (7). As a result of this effect, heat flux at early times comes down as the resistance increases. However, the total heat exchange over large time is fixed irrespective of the thermal contact resistance, i.e., the area under the heat flux vs time curve must remain constant. Therefore, heat flux catches up at large times and is greater in the presence of contact resistance compared to the perfect contact case. Fig. 8 shows similar impact of $\bar{R}$ on $\bar{q}_{12}$ for both quartz and aluminum.

Note that the value of $\bar{R}$ is usually obtained from the nature of the materials and the surface roughness, based on which, Fig. 8 can be used as a design tool to determine the heat flux to be expected as a function of time.

3.4. Limits for semi-infinite assumption to be reasonably accurate

While the finite thickness problem has been shown in previous sections to exhibit characteristics that are distinct from the semi-infinite problem, it is of interest to determine the regimes in which the body can be reasonably approximated to be semi-infinite. This is of particular practical importance because the semi-infinite solution is quite straightforward, given by Eqs. (1) and (2), whereas, the results of the finite thickness model, Eqs. (19) and (20) are more difficult to compute, as they involve calculating a number of eigenvalues and other coefficients.

Clearly, the larger the layer thickness $\bar{L}$, the more accurate would the semi-infinite assumption be. An estimate of the validity limit of this assumption may be obtained by calculating the thermal penetration depth up to a given time (which involves only the thermal diffusivity) and comparing against the thickness of the sample. However, this is merely an approximation that does not account for interaction between the two bodies. A more rigorous analysis of the validity of the semi-infinite assumption would require comparison of the semi-infinite solution, given by Eq. (2) with the solution for finite thickness, given by Eq. (20). This comparison is presented in Fig. 9, wherein the minimum thickness of a finite body needed for the semi-infinite assumption to be accurate within a given tolerance is plotted as a function of time. Plots are presented for four different tolerance levels – 5%, 10%, 15% and 20% – and for two different materials – quartz and aluminum –in contact with human skin. Fig. 9 presents these results in dimensional form, so as to serve as design guidelines for practical problems involving these materials. Similar plots for other material pairs can be easily generated based on Eqs. (2) and (20).

Fig. 9(a) and 9(b) show that the larger the time, the larger is the minimum thickness needed for accurate representation by the semi-infinite model. This is because the thermal diffusion wave propagates farther and farther with increasing time, thereby requiring greater thickness for the semi-infinite assumption to be valid. As expected, the tighter the tolerance demanded, the larger is the minimum layer thickness required for the semi-infinite assumption to be within tolerance. When comparing quartz and aluminum, it is found that for the same time and tolerance, the minimum thickness needed for quartz is much smaller – by nearly an order of magnitude – compared to aluminum. Further, it is found that making the tolerance tighter does not result in as much increase in the minimum thickness for the case of quartz as it does for aluminum. For example, in going from 20% tolerance to 5% tolerance, the minimum quartz thickness increases by only around 35%, whereas it goes up for aluminum by about 2.5 times. This is explainable on the basis of larger thermal diffusivity and effusivity of aluminum, due to which, a tighter tolerance presents a much more stringent requirement for aluminum than for quartz.

Note that the curves in Fig. 9 rise rapidly at first, and then slow down, which at first may appear indicative of a thermal penetration depth related $\sqrt{t}$ dependence of the minimum thickness needed. However, it is verified separately that a $\sqrt{t}$ curve does not accurately fit these results, indicating that the use of only the thermal penetration depth concept to estimate the minimum thickness

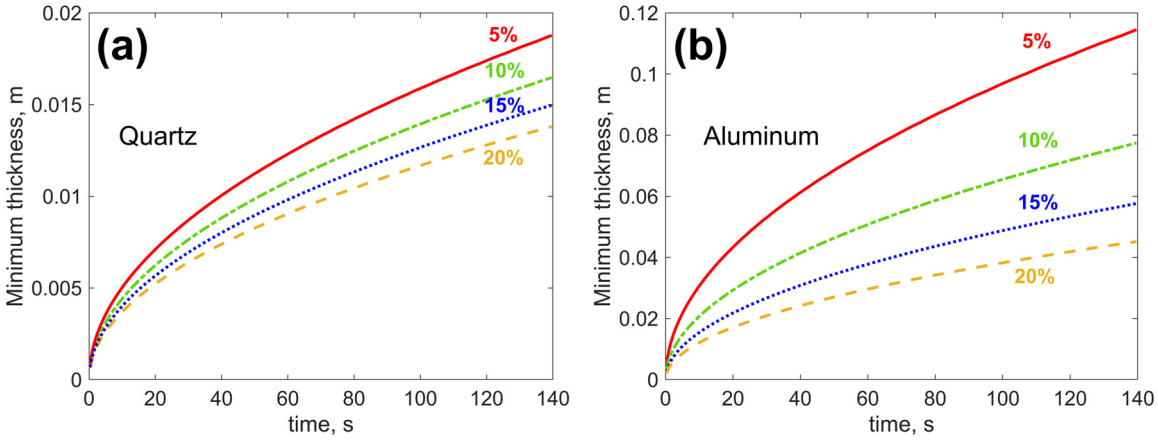

Fig. 9. Minimum thickness needed for a finite thickness body to be within a prescribed tolerance of the semi-infinite solution in terms of heat flux q_{12} as a function of time. 5%, 10%, 15% and 20% tolerance curves are plotted for two representative materials (a) quartz and (b) aluminum touching human skin.

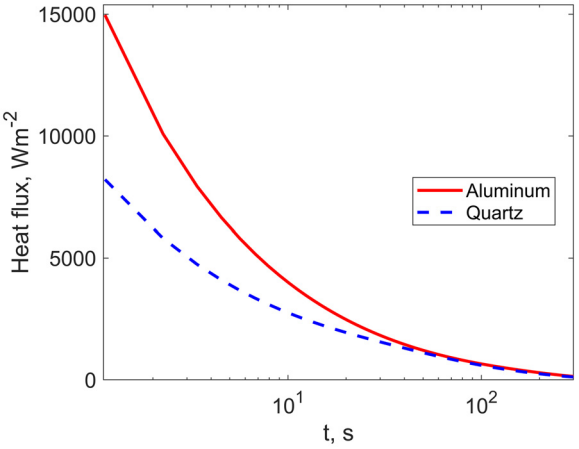

Fig. 10. Application of the analytical model for a dimensional problem: Heat exchanged between a human finger and a finite thickness body made of aluminum or quartz as a function of time. An initial temperature difference of 20 °C is assumed, and a thickness of each layer is assumed to be 1 cm.

needed is not accurate. Instead, a comprehensive comparison discussed above leads to more accurate results.

3.5. Practical applications

While much of the prior analysis in this work is presented in non-dimensional form for generality, it is also of interest to examine practical problems in dimensional form. In particular, it is of interest to calculate the heat flux in Wm^{-2} when a material such as quartz or aluminum comes in contact with human skin. This quantity is known to be correlated with the tactile sensation of warmth or coolness, which is usually the basis for interpreting thermal effusivity using the semi-infinite assumption. The finite thickness model developed in this work makes it possible to quantify the same effect when the two bodies are of finite thickness, as may be the case in several practical scenarios. To examine this further, Fig. 10 plots the dimensional interfacial heat flux as a function of time when a material of 1 cm thickness comes in contact with human skin of the same thickness, which may represent, for example, a finger tip. An initial temperature difference of 20 °C between the two bodies is assumed. Similar to the semi-infinite model, Fig. 9 shows that the finite thickness model also predicts greater heat flux – and therefore, a perception of coolness – for aluminum compared to quartz, which, due to lower heat flux, is expected to be perceived as warmer. While these results are qualitatively similar to the semi-infinite model, the use of the finite thickness model is quantitatively more accurate, particularly for metals, and at large times. In addition to human touch, the finite thickness model presented here may also be relevant for several other engineering problems, such as micromachines, geothermal energy and thermal energy storage.

4. Conclusions

Unlike other well-known thermophysical properties such as thermal conductivity, heat capacity and thermal diffusivity, there is much lesser work available on thermal effusivity. While the common understanding of thermal effusivity is on the basis of thermal contact between two semi-infinite bodies, the present work extends this to finite-sized bodies using multilayer diffusion analysis. Results presented here indicate that under certain conditions, the interfacial heat flux remains largely a function only of thermal effusivity and not any other property, similar to semi-infinite theory. The deviation mainly occurs in case of high thermal diffusivity/effusivity materials, at relatively large times and for small thicknesses. This insight may help design practical methods to measure thermal properties and to estimate the error involved in such measurements. Theoretical analysis presented in this work enhances the understanding of a practically important, but relatively less studied thermophysical property. Curves showing the minimum thickness needed for the semi-infinite assumption to be valid within a certain tolerance may be useful design tools for practical problems. These results may find applications in thermal property measurement techniques, as well as in a variety of engineering problems where thermal effusivity plays a key role.

Declaration of Competing Interest

None.

CRediT authorship contribution statement

Ankur Jain: Conceptualization, Methodology, Formal analysis, Investigation, Data curation, Visualization, Project administration, Writing – original draft, Writing – review & editing.

Data Availability

Data will be made available on request.

Acknowledgments

This material is partly based upon work supported by CAREER Award No. CBET-1554183 from the National Science Foundation.

References

[1] D.W. Hahn, M.N. Özışık, Heat Conduction, 3rd ed., Wiley, Hoboken, N.J., 2012 ISBN: ISBN: 978-0-470-90293-6.
[2] H.S. Carslaw, J.C. Jaeger, Conduction of Heat in Solids, Clarendon Press, Oxford, 1959.
[3] T.L. Bergman, D.P. Dewitt, A.S. Lavine, F.P. Incropera, 'Fundamentals of Heat and Mass Transfer,' John Wiley & Sons, New Jersey. ISBN: 978–0470501979
[4] E. Marín, Thermal physics concepts: the role of the thermal effusivity, Phys. Teach. 44 (2006) 432, doi:10.1119/1.2353583.
[5] T. Bhattacharjee, H.M. Clever, J. Wade, C.C. Kemp, Material recognition via heat transfer given ambiguous initial conditions,', IEEE Trans. Haptics 14 (2021) 885–896, doi:10.1109/TOH.2021.3089990.
[6] H. Hensel, K. Schafer, 'Thermoreception and temperature regulation in man,' In: E. Ring, B. Phillips (eds) Recent Advances in Medical Thermology, Springer, Boston, MA. doi: 10.1007/978-1-4684-7697-2_8.
[7] D.R. Kenshalo, C.E. Holmes, P.B. Wood, Warm and cool thresholds as a function of rate of stimulus temperature change, Percept Psychophys. 3 (1968) 81–84, doi:10.3758/BF03212769.
[8] A. Bouguerra, A. Ledhem, J.P. Laurent, M.B. Diop, M. Queneudec, Thermal effusivity of two-phase wood cement-based composites,', J. Phys. D Appl. Phys. 31 (1998) 2184, doi:10.1088/0022-3727/31/17/017.
[9] S.S. Pavlović, S.B. Stanković, D.M. Popović, G.B. Poparić, Transient thermal response of textile fabrics made of natural and regenerated cellulose fibers, Polym. Test. 32 (2014) 97–102, doi:10.1016/j.polymertesting.2013.12.010.
[10] W. Yang, P. Lu, Y. Chen, Laboratory investigations of the thermal performance of an energy pile with spiral coil ground heat exchanger, Energy Build. 128 (2016) 491–502, doi:10.1016/j.enbuild.2016.07.012.
[11] A.L. Cottrill, A.T. Liu, Y. Kunai, V.B. Koman, A. Kaplan, S.G. Mahajan, P. Liu, A.R. Toland, M.S. Strano, Ultra-high thermal effusivity materials for resonant ambient thermal energy harvesting, Nat. Commun. 9 (2018) 664, doi:10.1038/s41467-018-03029-x.
[12] G. Liang, J. Zhang, S. An, J. Tang, S. Ju, S. Bai, D. Jiang, Phase change material filled hybrid 2D /3D graphene structure with ultra-high thermal effusivity for effective thermal management, Carbon 176 (2021) 11–20 N Y, doi:10.1016/j.carbon.2020.12.046.
[13] Y.K. Koh, D.G. Cahill, Frequency dependence of the thermal conductivity of semiconductor alloys, Phys. Rev. B 76 (2007) 075207, doi:10.1103/PhysRevB.76.075207.
[14] E. Marín, The role of thermal properties in periodic time-varying phenomena, Eur. J. Phys. 28 (2007) 429, doi:10.1088/0143-0807/28/3/005.
[15] S.E. Gustafsson, 'On the development of the hot strip, hot disc, and pulse hot strip methods for measuring thermal transport properties,' In: Proceedings of the 32nd International Thermal Conductivity Conference, 2015, West Lafayette, IN, USA. doi: 10.5703/1288284315537.
[16] S.E. Gustafsson, Transient plane source techniques for thermal conductivity and thermal diffusivity measurements of solid materials, Rev. Sci. Instrum. 62 (1991) 797, doi:10.1063/1.1142087.
[17] M. Emanuel, 'Effusivity sensor package (ESP) system for process monitoring and control,' In: Proceedings of the 28th International Thermal Conductivity Conference, St. Andrews by-the-Sea, NB, Canada, 2005. Available at https://memanuel.files.wordpress.com/2010/08/mathis_effusivity_sensor_technology3.pdf, last accessed 10/17/2022.
[18] M. Emanuel, B.C. Brown, S.L.G. Ackermann, R. Bateman, MTPS analytical temperature and heat flux solution with thermal contact resistance, J. Heat Transf. 144 (2022) 071401, doi:10.1115/1.4054383.
[19] M. Gustavsson, E. Karawacki, S.E. Gustafsson, Thermal conductivity, thermal diffusivity, and specific heat of thin samples from transient measurements with hot disk sensors, Rev. Sci. Instrum. 65 (1994) 3856, doi:10.1063/1.1145178.
[20] Y. Jannot, P. Meukam, Simplified estimation method for the determination of the thermal effusivity and thermal conductivity using a low cost hot strip, Meas. Sci. Technol. 15 (2004) 1932–1938, doi:10.1088/0957-0233/15/9/034.
[21] K. Hatori, N. Taketoshi, T. Baba, H. Ohta, Thermoreflectance technique to measure thermal effusivity distribution with high spatial resolution,', Rev. Sci. Instrum. 76 (2005) 114901, doi:10.1063/1.2130333.
[22] M. Ryu, J.-C. Batsale, J. Morikawa, Quadrupole modelling of dual lock-in method for the simultaneous measurements of thermal diffusivity and thermal effusivity, Int. J. Heat Mass Transf. 162 (2020) 120337, doi:10.1016/j.ijheatmasstransfer.2020.120337.
[23] U. Zammit, F. Mercuri, S. Paoloni, M. Marinelli, R. Pizzoferrato, Simultaneous absolute measurements of the thermal diffusivity and the thermal effusivity in solids and liquids using photopyroelectric calorimetry, J. Appl. Phys. 117 (2015) 105104, doi:10.1063/1.4914491.
[24] S. Oss, A simple model of thermal conduction in human skin: temperature perception and thermal effusivity, Eur. J. Phys. 43 (2022) 035101, doi:10.1088/1361-6404/ac4c8a.
[25] C.W. Tittle, Boundary value problems in composite media: quasi-orthogonal functions, J. Appl. Phys. 36 (1965) 1486–1488, doi:10.1063/1.1714335.